EDINBURGH INSTRUMENTS

50 YEARS 1971-2021

PRECISION RAMAN

Best-in-class Raman microscopes
for research and analytical requirements backed with world-class customer support and service.

edinst.com

Research Article

Journal of RAMAN SPECTROSCOPY

Received: 28 July 2009 Accepted: 14 October 2009 Published online in Wiley Online Library: 13 January 2010

(wileyonlinelibrary.com) DOI 10.1002/jrs.2562

Molecular structure, spectroscopic (FTIR, FTIR gas phase, FT-Raman) first-order hyperpolarizability and HOMO–LUMO analysis of 4-methoxy-2-methyl benzoic acid

C. Meganathan,[a] S. Sebastian,[b] M. Kurt,[c] Keun Woo Lee[a] and N. Sundaraganesan[b]*

Vibrational spectral analysis was carried out for 4-methoxy-2-methyl benzoic acid (4M2MBA) by using Fourier transform infrared (FT-IR) (solid, gas phase) and FT-Raman spectroscopy in the range of 400–4000 and 10–3500 cm^{-1} respectively. The effects of molecular association through O–H···O hydrogen bonding have been described by the single dimer structure. The theoretical computational density functional theory (DFT) and Hatree-Fock (HF) method were performed at 6–311++G(d,p) levels to derive the equilibrium geometry, vibrational wavenumbers, infrared intensities and Raman scattering activities. The scaled theoretical wavenumbers were also shown to be in good agreement with experimental data. The first-order hyperpolarizability (β_0) of this novel molecular system and related properties (β, α_0 and $\Delta\alpha$) of 4M2MBA are calculated using the B3LYP/cc-pvdz basis set, based on the finite-field approach. A detailed interpretation of the infrared and Raman spectra of 4M2MBA is reported. The theoretical spectrograms for FT-IR and FT-Raman spectra of the title molecule were also constructed and compared with the experimental one.

Supporting information may be found in the online version of this article.

Keywords: vibrational spectra; FTIR spectra; FT-Raman spectra; dimer; first-order hyperpolarizability; HOMO–LUMO

Introduction

The derivatives of benzoic acids are biologically active substances and are constituents of vitamin B-complex.[1] They are also essential organic compound constituents of lenticular pigments present in the eye lenses of humans and in certain diurnal animals.[2] Benzoic acid is widely found in plants and animals and is used in miticides, as contrast media in urology, for cholocystrographic examination and in the manufacture of pharmaceuticals. It also finds application in dyes, in curing tobacco, in preserving fruit juices, in many esters, as a mordant in cloth printing and as a reference standard in volumetric analysis. Benzoic acid derivatives are used in medicine as a protective drug against UV radiation in the diagnosis of gastrointestinal disorders and therapeutically in fibrotic skin disorders.[3]

Benzoic acid derivatives play a useful role in mosquito control by maintaining the vector population at a minimum level.[4] Some of the benzoic acid derivatives find use as intermediate compounds for a continuous spectrometric assay of conjugated bile acid hydrolase.[5] Benzoic acid is used as an antifungal agent for superficial fungus infection of skin. Together with salicylic acids in ointments, it is also used for the treatment of ring worm in dogs and other species.[6]

Para-chlorobenzoic acid, one of the fastest reacting and higher melting acids, and organic materials such as 4-aminobenzoic acid possess excellent UV ray absorption ability and they have been used as sun care products.[7] Because of their wide applications, the surface-enhanced Raman scattering studies,[8] vibrational spectra of benzoic acid[9] and nitro derivatives have been extensively investigated. Verma *et al*.[10] studied the infrared absorption spectrum of *m*-fluorobenzoic acid with the help of nujol mull in the region of 250–4000 cm^{-1}. The assignments of the fundamentals were proposed for this compound by assuming the C_s symmetry. The Stokes as well as anti-Stokes laser Raman spectra of 2,3,5-tri-iodobenzoic acid[11] have been recorded in the region of 150–4000 cm^{-1}. Fourier transform infrared (FT-IR) spectra of the above-mentioned compound have also been recorded in the solid phase as well as liquid phase in the region of 400–4000 cm^{-1}. The vibrational analysis has been carried out by assuming C_s point group symmetry.

Rastogi *et al*.[12] recorded and studied the infrared absorption spectra of 2-chloro-5-nitrobenzoic and 3,5-dinitrobenzoic acids

* *Correspondence to: N. Sundaraganesan, Department of Physics (FEAT), Annamalai University, Annamalainagar 608 002, Tamilnadu, India. E-mail: sundaraganesan_n2003@yahoo.co.in*

a *Division of Applied Life Science (BK21 Program), Environmental Biotechnology National Core Research Center (EB-NCRC), Plant Molecular Biology and Biotechnology Research Center (PMBBRC), Gyeongsang National University, Jinju 660-701, Republic of Korea*

b *Department of Physics (FEAT), Annamalai University, Annamalainagar 608 002, Tamilnadu, India*

c *Ahi Evran Öniversitesi Fen Edebiyat Fakültesi Fizik Bölömö, Asıkpasa Kampusö, 40100 Kirsehir-Turkiye, Turkey*

in the solid phase in the region of 200–4000 cm^{-1}. The spectra have been analysed assuming C_s point group symmetry and observed fundamentals have been assigned to different normal modes of vibrations. Ahamed *et al.*[13] recorded the laser Raman and FT-IR spectra of 3,5-dinitrobenzoic acid in the regions of 250–4000 and 50–4000 cm^{-1} respectively. Recently, we[14] have investigated the structure, harmonic wavenumbers and vibrational mode assignments for 2-chlorobenzoic acid monomer using HF and density functional theory (DFT) methods employing the 6-311++G(d,p) basis set. A literature survey reveals that to the best of our knowledge no *ab initio* HF/DFT wavenumber and structural parameter calculation of 4-methoxy-2-methylbenzoic acid (4M2MBA) has been reported so far. Therefore, the present investigation was undertaken to study the vibrational spectra, highest occupied molecular orbital (HOMO), lowest unoccupied molecular orbital (LUMO) analysis and first-order hyperpolarizability of this non linear optics (NLO) active molecule completely and to identify the various normal modes with greater wavenumber accuracy.

Experimental

The compound 4M2MBA in the solid form was purchased from Sigma–Aldrich Chemical Company (USA), with a stated purity of greater than 98% and it was used as such without further purification. The FT-Raman spectrum of 4M2MBA has been recorded using the 1064-nm line of an Nd:YAG laser as excitation wavelength in the region of 10–3500 cm^{-1} on a Brucker model IFS 66V spectrophotometer equipped with an FRA 106 FT-Raman module accessory. The FT-IR gas-phase spectrum was also recorded by gas chromatography coupled to an FT-IR instrument (Brucker, vector). The FT-IR spectrum of this compound was recorded in the range of 400–4000 cm^{-1} on an IFS 66 V spectrophotometer using the KBr pellet technique. The spectrum was recorded at room temperature, with a scanning speed of 10 cm^{-1} min^{-1} and a spectral resolution of 2.0 cm^{-1}. The observed experimental FT-IR (solid and gas) and FT-Raman spectra along with the theoretical spectra are shown in Figs 1–4. The spectral measurements were carried out at the Central Electrochemical Research Institute (CECRI), Karaikudy, Tamil Nadu, India.

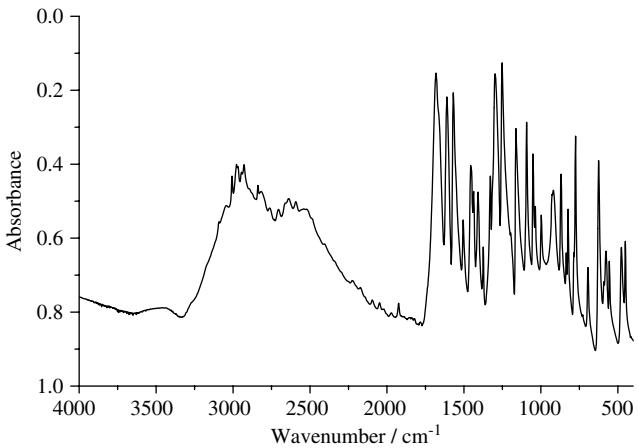

Figure 1. FT-IR (solid phase) spectrum of 4-methoxy-2-methylbenzoic acid.

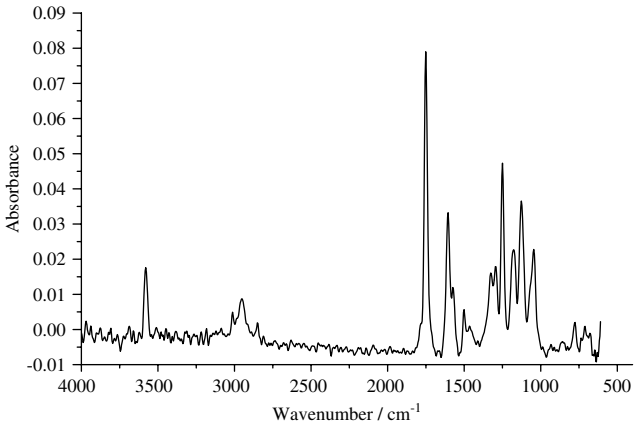

Figure 2. FT-IR (gas phase) spectrum of 4-methoxy-2-methylbenzoic acid.

Computational Details

The first task of the computational work was to determine the optimized geometry of the compound. Both the geometry optimizations and wavenumber calculations for 4M2MBA monomer and dimer were carried out using both *ab initio* HF and the hybrid density functional B3LYP (Becke–Lee–Young–Parr composite of exchange correlation) functional with the 6-311++G(d,p) basis set, using the Gaussian 03 W[15] program package, invoking gradient geometry optimization.[16] Geometries of the model 4M2MBA have been first optimized with full relaxation on the potential energy surfaces at the HF/6-31G(d,p) level and the resultant geometries have been used as inputs for further calculations at the DFT(B3LYP) level. Polarization functions have been added for the better treatment of the methoxy, methyl and carboxyl groups. Analytic frequency calculations at the optimized geometry were done to conform the optimized structure to be an energy minimum and to obtain the theoretical vibrational spectra. The total energy distribution (TED) was calculated by using the scaled quantum mechanics (SQM) program[17,18] and the fundamental vibrational modes were characterized by their TED.

Prediction of Raman intensities and hyperpolarizability

The Raman activities (S_i), calculated with the Gaussian 03 program,[15] were converted to relative Raman intensities (I_i) using the following relationship derived from the intensity theory of Raman scattering.[19,20]

$$I_i = \frac{f(v_o - v_i)^4 S_i}{v_i[1 - \exp(-hcv_i/kt)]} \quad (1)$$

where ν_o is the exciting wavenumber in cm^{-1}, ν_i the vibrational wavenumber of the *i*th normal mode, *h*, *c* and *k* are fundamental constants and *f* is a suitably chosen common normalization factor for all peak intensities. For simulation, calculated FT-Raman spectra have been plotted using pure Lorentzian band shape with a bandwidth (FWHM) of 10 cm^{-1}, as shown in Fig. 4.

The first hyperpolarizability (β_0) of this novel molecular system and related properties (β, α_0 and $\Delta\alpha$) of 4M2MBA are calculated using the CC/PVDZ/6-31G(d,p) basis set, based on the finite-field approach. In the presence of an applied electric field, the energy of a system is a function of the electric field. First, hyperpolarizability is a third-rank tensor that can be described by a $3 \times 3 \times 3$ matrix. The

Journal of RAMAN SPECTROSCOPY

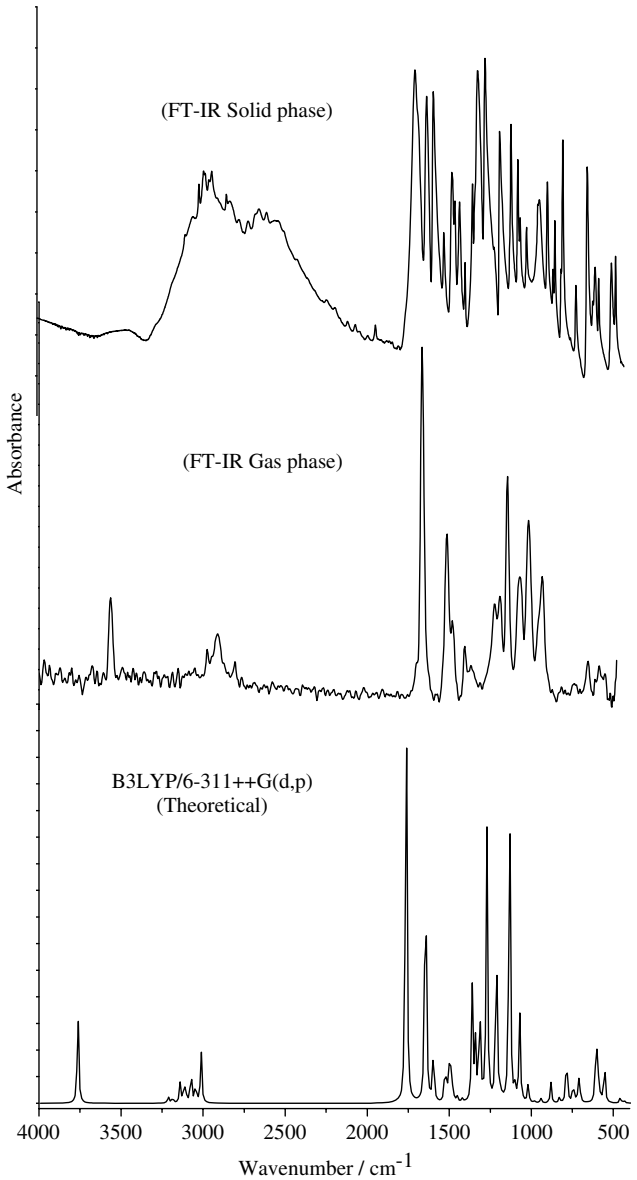

Figure 3. Comparison of observed and computed FT-IR spectrum of 4-methoxy-2-methylbenzoic acid.

27 components of the 3D matrix can be reduced to 10 components due to the Kleinman symmetry.[21] It can be given in the lower tetrahedral format. It is obvious that the lower part of the $3 \times 3 \times 3$ matrixes is a tetrahedral. The components of β are defined as the coefficients in the Taylor series expansion of the energy in the external electric field. When the external electric field is weak and homogeneous, the expansion becomes

$$E = E^0 - \mu_\alpha F_\alpha - 1/2\alpha_{\alpha\beta}F_\alpha F_\beta - 1/6\beta_{\alpha\beta\gamma}F_\alpha F_\beta F_\gamma + \cdots \quad (2)$$

where E^0 is the energy of the unperturbed molecules, F_α is the field at the origin and μ_α, $\alpha_{\alpha\beta}$ and $\beta_{\alpha\beta\gamma}$ are the components of dipole moment, polarizability and the first hyperpolarizabilities respectively. The total static dipole moment μ, the mean polarizability α_0, the anisotropy of the polarizability $\Delta\alpha$ and the mean first hyperpolarizability β_0, using the x, y, z components, are

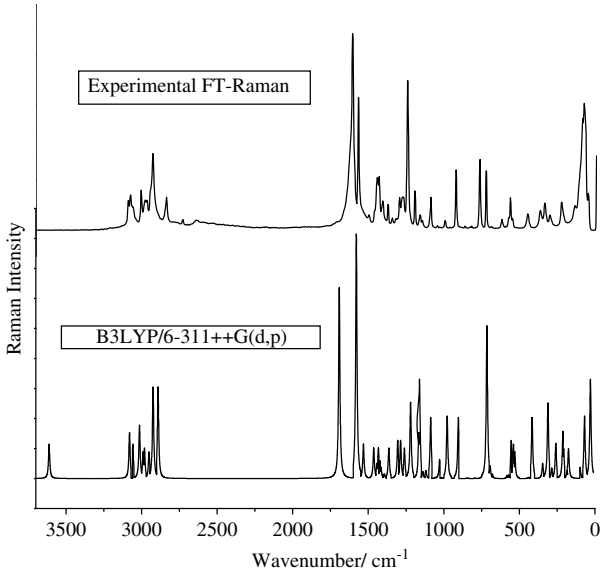

Figure 4. Comparison of observed and computed FT-Raman spectrum of 4-methoxy-2-methylbenzoic acid.

defined as

$$\mu = (\mu^2{}_x + \mu^2{}_y + \mu^2{}_z)^{1/2} \quad (3)$$

$$\alpha_0 = \frac{\alpha_{xx} + \alpha_{yy} + \alpha_{zz}}{3} \quad (4)$$

$$\alpha = 2^{-1/2}[(\alpha_{xx} - \alpha_{yy})^2 + (\alpha_{yy} - \alpha_{zz})^2 + (\alpha_{zz} - \alpha_{xx})^2 + 6\alpha^2 xx]^{1/2} \quad (5)$$

$$\beta 0 = (\beta^2{}_x + \beta^2{}_y + \beta^2{}_z)^{1/2} \quad (6)$$

and

$$\beta_x = \beta_{xxx} + \beta_{xyy} + \beta_{xzz} \quad (7)$$

$$\beta_y = \beta_{yyy} + \beta_{xxy} + \beta_{yzz} \quad (8)$$

$$\beta_z = \beta_{zzz} + \beta_{xxz} + \beta_{yyz} \quad (9)$$

The total molecular dipole moment and mean first hyperpolarizability of 4M2MBA are 2.925 Debye and 1.5×10^{-30} esu respectively, as shown in Table S1 (Supporting Information). The total molecular dipole moment (μ) and mean first hyperpolarizability (β) are given directly as 2.9215 Debye and 1.5×10^{-30} esu respectively, as shown in Table S1 (Supporting Information). The total dipole moment of the title molecule is approximately two times greater than that of urea and the first hyperpolarizability of title molecule is four times greater than that of urea (μ and β of urea are 1.3732 Debye and 0.3728×10^{-30} esu obtained by the HF/6-31G(d,p) method).

Results and Discussions

Molecular geometry

The numbering of atoms for monomer and dimer is given in Fig. 5(a) and (b). The optimized geometrical parameter bond lengths and bond angles by *ab initio* HF, DFT/B3LYP with 6-311++G(d,p) as the basis set are listed in Table S2 (Supporting Information). As the crystal structure of the exact title compound is not available as yet, the optimized structure can only be compared

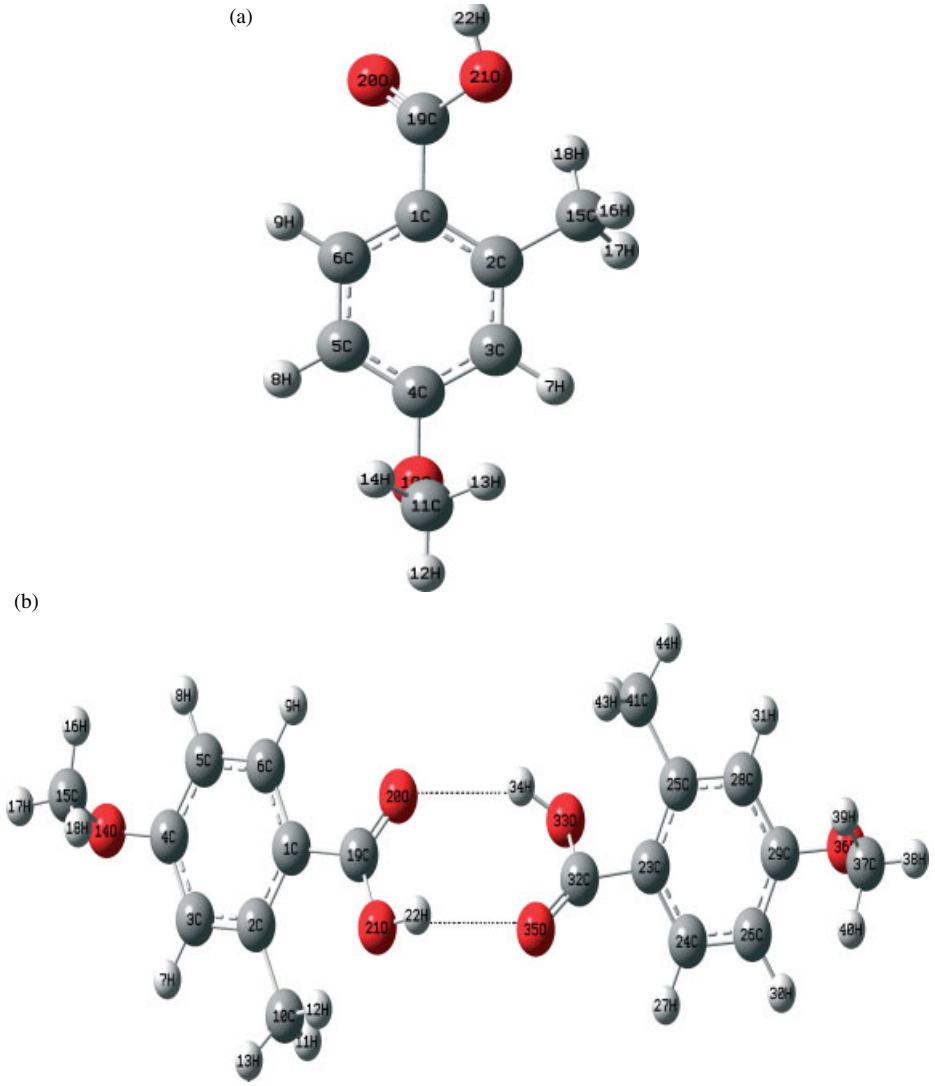

Figure 5. (a) Atom numbering system adopted in this study for 4-methoxy-2-methylbenzoic acid; (b) dimer structure of 4-methoxy-2-methylbenzoic acid.

with other similar systems for which the crystal structures have been solved, e.g. 2,6-dimethoxy benzoic acid.[22] As seen from Table S2 (Supporting Information), most of the optimized bond lengths are slightly longer than the experimental values, and the bond angles are slightly different from experimental ones because the molecular states are different during experimental and theoretical processes. One isolated molecule is considered in the gas phase during theoretical calculation, while many packing molecules are treated in the condensed phase during the experimental measurements.

In the title molecule studied here, the introduction of three substituent groups on the benzene ring causes some changes in the ring C–C bond distances and also in the position of the substituents in the benzene ring. Also, its electron donor/acceptor capabilities play a very important role in shaping the structural and electronic properties of the molecules. The methyl groups are referred to as *electron-donating substituents* in the aromatic ring system. The methyl group shares its loan pair electrons with the p electrons in a ring and the methyl group interacts with the nearby π systems. The methyl and phenoxy groups may produce intramolecular interactions with carboxylic acid and the H atom in the meta position. This interaction can affect the regular hexagonal structure, as is evident from calculated bond angles shown in Table S2 (Supporting Information), i.e. C2–C1–C6 and C3–C4–C5 are 119.08° and 119.66°; the same effect is also observed on the other side of the ring, as shown in Table S2 (Supporting Information).

The C–C bond distances vary by 0.01 Å in the most extreme cases within the same method of calculations. Thus, e.g. the shortest C–C bond of 1.381 Å was calculated by using the HF/6-311++G(d,p) method, whereas the longest C–C bond was calculated as 1.421 Å by using the B3LYP/6-311++G(d,p) method. These values are in good agreement with the data obtained for substituted benzenes.[23] For example, in nicotinic acid, the shortest C–C bond was 1.383 Å, while the longest was 1.406 Å. In the carboxylic group, the calculated value C_{aro}–C19 is in the region of 1.486 Å by the HF/6-311++G(d,p) method and 1.484 Å by the B3LYP/6-311++G (d,p) method, which are in excellent agreement with the experimental value of 1.485 Å. The C_{19}–O_{20} bond length calculated at 1.213 Å by the B3LYP/6-311++G(d,p) method is in good agreement with the literature structural data.[24–26] The calculated C_{19}–O_{21} bond distance in 4M2MBA is characteristic of the C–O (H) bond length, which is not involved in the hydrogen-

bonding system and has a value in the range of 1.329–1.360 ´Å by both methods.

Although theoretical results are not exactly close to the experimental values for the compound, it is generally accepted that bond lengths and bond angles depend on the method and the basis set used in the calculations; the calculated geometric parameters also represent good approximations and can be used as a foundation to calculate the other parameters for the compounds.

Hydrogen bonding

The structures show the presence of inter-molecular hydrogen bond interaction in 4M2MBA, as shown in Fig. 5(b). In our present study, the hydrogen bond analysis has been carried out by the B3LYP/6-311++G(d,p) method, as shown in Table S2 (Supporting Information). The weak hydrogen bond type of interaction between O21···H22–O35 and O33–H34···O20 is observed and the distance between O21···O35 and 033···O20 is about 3.055 and 3.066 Å respectively; the above are well within the range of <3.0 Å for hydrogen interaction.[27] The other parameters, i.e the bond angles between the hydrogen bonding are also shown in Table S2 (Supporting Information).

Vibrational analysis

The molecule 4-methoxy-2-methylbenzoic acid is a trisubstituted aromatic system. The vibrational bands observed in the infrared region are very sharp, broad and less intense. According to the theoretical calculations, the 4M2MBA possesses a planar structure of C_s point group symmetry. In this point group, two types of vibrations occur, namely symmetric ($A^{/}$) and antisymmetric ($A^{//}$). All the 60 fundamental vibrations are active in both IR absorption and Raman scattering.

The observed and calculated vibrational wavenumbers using HF and DFT(B3LYP/6-311++G(d,p), along with their relative intensities and Raman scattering activities, are given in Table 1. In the last column, a detailed description of the normal modes based on the TED is given. Furthermore, none of the predicted vibrational spectra have any imaginary wavenumber, implying that the optimized geometry is located at the local lowest point on the potential energy surface. We know that *ab initio* HF and DFT potentials systematically overestimate the vibrational wavenumbers. These discrepancies are corrected by computing anharmonic corrections explicitly, by introducing a scaled field[28] or directly scaling the calculated wavenumbers with the proper factor.[29] Considering systematic errors with scaling factors of 0.96 and 0.89, we calibrated the vibrational wavenumbers calculated by the B3LYP and HF methods. After scaling with a scaling factor, the deviation from the experiments was less than 10 cm^{-1}, with few exceptions.

C–H vibrations

The heteroaromatic structure shows the presence of C–H stretching vibration in the region of 3100–3000 cm^{-1}, which is the characteristic region for the ready identification of C–H stretching vibration.[30,31] In this region, the bands are not affected appreciably by the nature of the substituent. As the 4M2MBA is a trisubstituted aromatic system, it has one isolated and two adjacent C–H moieties. The three expected C–H stretching vibrations correspond to stretching modes of C_3–H, C_5–H and C_6–H units. Hence, in our present work, the FT-Raman band observed at 3077 cm^{-1} is assigned to a C–H stretching vibration. The scaled vibration (mode nos: 59–57) by the B3LYP/6-311++G(d,p) method predicted at 3106, 3091 and 3080 cm^{-1} shows very good agreement with recorded spectral data. The HF level after scaling down gives wavenumber values of 3072, 3057 and 3046 cm^{-1}, and mode numbers 54–57 (Table 1) are assigned to the C–H stretching vibration. As expected, these modes are pure stretching modes as evident from the TED column; they contribute l00%.

The in-plane aromatic C–H bending vibration occurs in the region of 1300–1000 cm^{-1}; the bands are sharp but have weak-to-medium intensity. The C–H in-plane bending vibration computed at 1270, 1229 and 1175 cm^{-1} (mode nos: 37–35) by the B3LYP method shows excellent agreement with FT-IR bands at 1251, 1248 and 1199 cm^{-1} in the FT-Raman and 1249 cm^{-1} in the FT-IR gas phase.

The bands observed at 853 and 775 cm^{-1} in FT-IR (gas phase) and 869, 834 and 774 cm^{-1} in FT-IR solid phase are assigned to C–H out-of-plane bending vibrations for 4M2MBA. This also shows good agreement with theoretically scaled harmonic wavenumber values at 851, 801 and 759 cm^{-1} by the B3LYP method.

O–CH_3 group vibrations

The C–H stretching vibrations in the methoxy group of bands observed in FT-IR (solid phase) at 2977, 2828, 2838 cm^{-1} and 2853 cm^{-1} in FTIR (gas phase) and FT-Raman values at 2971, 2929 and 2838 cm^{-1} are assigned to C–H asymmetric and symmetric stretching vibrations. The TED corresponding to these vibrations contributes 100% without any contribution from other vibrations, as shown in Table 1. The theoretically scaled values (mode nos: 51–53) are also in good agreement with the experimental values. The theoretically predicted value of 1454 cm^{-1} by the B3LYP/6-311++G(d,p) method (mode no: 46) is assigned to the CH_3 deformation mode and is in good agreement with the experimental value of 1455 cm^{-1} in FTIR (solid phase) and 1461 cm^{-1} in FTIR (gas phase). The calculated TED for the CH_3 deformation is only 63% and this mode is combined with other vibrations, as shown in Table 1. The very strong band at 1129 cm^{-1} in FTIR (gas phase) assigned as CH_3 twisting vibration is in excellent agreement with the theoretically calculated value by the B3LYP/6-311++G(d,p) method at 1127 cm^{-1} (mode no: 32). The vibrational wavenumbers at 235 and 143 cm^{-1} in FT-Raman are assigned to the CH_3 in-plane bending vibration and the out-of-plane bending vibration respectively. The O–CH_3 vibration mode is assigned at ~1040 cm^{-1} for anisole[32] and in the region of 1000–1100 cm^{-1} for anisole and its derivatives.[33–36] This mode is assigned at 1026, 909 and 995 cm^{-1} for *o*-, *m*- and *p*-methoxy benzaldehydes, respectively. In our case, the O–CH_3 stretching mode is assigned to a weak FT-IR band at 1050 cm^{-1} (solid phase) and at 1044 cm^{-1} FT-IR band (gas phase). The theoretically computed value at 1062 cm^{-1} (mode no: 30) coincides with the experimental results. The C–O–CH_3 angle bending mode has been assigned close to 300 cm^{-1} for anisole by Owen and Hester[37] and at 421 cm^{-1} for *p*-methoxy benzaldehyde by Campaqnaro and Wood.[38] Rao *et al.*[33–36] have proposed an assignment for this mode in the region of 300–670 cm^{-1} for anisole and its derivatives. As this mode lies in the region of the ring planar C–C–C angle bending modes, a strong mixing amongst these two modes and other planar modes is expected. Singh and Yadav[39] assigned the C–O–CH_3 angle bending mode at 341, 382 and 430 cm^{-1} for the

Table 1. Vibrational wavenumbers obtained for 4M2MBA at HF/6-311++G(d,p) and B3LYP/6-311++G(d,p) [harmonic frequency (cm^{-1}), IR intensities (km mol^{-1}), Raman scattering activities ($Å^4$ amu^{-1})]

	Experimental (cm^{-1})			Calculated wavenumbers (cm^{-1})		IR intensity		Raman scattering activity		
Mode no.	FTIR (solid)	FTIR (gas)	FT-Raman	HF/6-311++G(d,p)	B3LYP/6-311++G(d,p)	HF/6-311++G(d,p))	B3LYP/6-311++G(d,p)	HF/6-311++G(d,p)	B3LYP/6-311++G(d,p)	Characterizations of normal modes with TED
1				32	30	0	0	0	0	ΓOCCC (91)
2			54 w	68	69	0	0	0	0	ΓCCC0 (10)+ ΓCOCC (53)+ ΓCCCC (10)
3				102	100	1	1	0	0	ΓCCCC (36)+ ΓCOCC (34)
4			143 w	178	176	1	1	0	1	γOCC (28)+ γCCO (16)+ γCOC (14)+ γCCC (19)
5				198	186	0	0	0	0	ΓCCCC (17)+ Γ HCCC(64)
6				222	208	0	0	0	1	ΓHCOC (58)
7			235 w	228	214	0	0	1	1	ΓCCCC (26)+ ΓHCCC (28)+ ΓHCOC (22)
8				261	261	0	0	1	1	γOCC (23)+ γCCO (10)+ γCOC (21)+ γCCC (30)
9				300	288	0	1	0	0	ΓCCCC (23)+ ΓOCCC (24)+ ΓCCCO (12)+ ΓHCOC(17)
10			306 w	314	313	0	1	2	4	νCC (12)+ γCCC (45)
11			344 w	349	348	0	0	0	1	νCC (20)+ γCCC (40)+ γOCC (10)
12				421	419	1	1	2	5	νCC (14)+ γOCC (37)+ γCOC (21)
13	451 w		457 w	455	442	1	1	0	0	
14				542	535	12	9	1	3	ΓHOCC (33)+ ΓHOCO (11)
15				544	542	0	1	2	4	νCC (15)+ γ CCC (38)
16	555 w			564	558	1	1	2	5	γCCC (29)+ γOCC (28)
17	576m		579m	591	575	3	8	0	1	ΓCCCC (10)+ ΓHCCC (10)+ ΓHOCC (26)+ ΓHOCO(19)
18				593	585	12	15	0	0	γCCC (14)+ γCCO (13)+ γCOC (12)+ γOCO (16)
19	669 w			704	684	4	7	0	1	ΓCCCC (36)+ ΓHCCC(12)+ ΓCCCH (13)+ ΓOCCC(10) + ΓHOCO (11)
20	694m			711	699	0	1	1	2	νCC (16)+OC (23)+ γCCC (15)+ γOCO (12)
21	726s	730	720	8	5	13	26			νCC (43)
22	774s	775 w	771s	796	759	15	12	0	0	ΓHCCC (10)+ ΓOCCC (36)+ ΓHOCO (19)
23	834 w			839	801	0	1	0	0	ΓHCCC (29)+ ΓHCCO (21)+ ΓCCCH (18)+ ΓOCCC (13)
24	869m	853 w		879	851	5	4	0	0	ΓHCCC (38)+ ΓCCCH (12)+ ΓOCCH (28)
25	918m			919	911	1	1	6	6	νCC (35)+ νOC,CO (29)+ γCCC (12)
26		931 w	926s	1000	948	0	0	0	0	ΓHCCC (46)+ ΓHCCH (37)
27	997 w		1001 w	1002	985	1	4	2	1	νCC (17)+ νCO (14)+ γHCC (39)+ ΓHCCC (15)
28				1052	1023	1	1	0	0	HCC (63)+ ΓHCCC (30)
29	1036 w			1056	1036	5	20	6	3	νCC (18)+ νCO (26)+ γHCC (15)
30	1050s	1044s		1096	1062	6	3	6	0	νCO (19)+ νOC (31)
31	1092s		1093m	1126	1095	25	73	1	9	νCC (19)+ νOC (12)+ γCCH (14)+ γHCC (17)

Table 1. (*Continued*)

Mode no.	Experimental (cm^{-1}) FTIR (solid)	FTIR (gas)	FT-Raman	Calculated wavenumbers (cm^{-1}) HF/6-311++G(d,p)	B3LYP/6-311++G(d,p)	IR intensity HF/6-311++G(d,p))	B3LYP/6-311++G(d,p)	Raman scattering activity HF/6-311++G(d,p)	B3LYP/6-311++G(d,p)	Characterizations of normal modes with TED
32			1129 vs	1145	1127	12	0	7	1	γHCO (85)+ ΓHCOC (13)
33				1162	1148	0	2	1	1	νCC (12)+ γHCC (20)+ γHCO (29)
34	1161s	1178s	1163 w	1176	1170	0	15	3	17	νCC (27)+ γHCO (25)+ γHOC (15)
35			1199s	1206	1175	43	24	17	8	νCC (17)+ γHCC (18)+ γCCH(12)+ γHOC(21)
36				1219	1229	7	60	4	13	νCC (19)+OC (18)+HCC (27)
37	1251 vs	1249 vs	1248 vs	1262	1270	49	25	14	6	νCC (12)+ νOC (20)+ γHCC(26) + γCCH (17)
38	1297 vs	1291 w	1304 w	1304	1295	39	13	13	8	νCC (80)
39	1328s	1327 w		1354	1314	32	25	11	7	νCC (14)+ νOC (21)+ γHOC (31)
40	1371m		1376 w	1404	1373	0	1	3	5	γHCC (42)+HCH (51)
41	1408s		1410m	1429	1404	1	1	1	1	νCC (30)+ γHCC (11)
42				1459	1426	1	1	2	2	γHCO (43)+ γHCH (43)
43				1460	1432	1	2	5	4	γHCC (12)+ γHCH (56)+HCCC (20)
44				1465	1443	5	2	1	7	γHCH (69)+ΓHCOC (22)
45			1435m	1473	1444	1	7	8	1	γHCC (14)+ γHCH(41)+ ΓHCCC (18)
46	1455s	1461 w		1480	1454	4	7	5	4	γHCO (12)+ γHCH(63)+ ΓHCOC (17)
47	1507s	1503 w	1502 w	1508	1474	8	9	4	7	νCC (30)+ γHCC (25)
48	1568 vs	1573 vs	1581	1543	15	13	14	9		νCC (60)
49	1610 vs	1602 vs	1612 vs	1623	1590	57	65	69	67	νCC (65)+ γHCC (10)
50	1750 vs	1768	1704	100	100	33	61			νOC (80)
51	2838 w	2853 w	2838m	2881	2912	9	13	80	84	νCH (100)
52	2928m	2929s	2903	2945	4	4	100	100		νCH (100)
53	2977 w	2971 w	2939	2972	7	7	25	29		νCH (100)
54	2964	3002	4	2	36	35				νCH (100)
55	3006 w	3015 w	3007m	2964	3011	3	4	39	30	νCH (100)
56	2988	3035	6	4	75	64				νCH (100)
57	3046	3080	1	1	47	42				νCH (100)
58	3057	3091	0	0	22	21				νCH (100)
59	3077m	3072	3106	1	2	61	55			νCH (100)
60	3354 br, sh	3574 ms	3743	3638	28	22	57	70		νOH (100)

brsh, broad shoulder; w, weak; vw, very weak; m, medium; ms, medium-strong; s, strong; vs, very strong; ν, tretching; γ, bending; Γ, torsion.

Journal of RAMAN SPECTROSCOPY

o-, *m*- and *p*-methoxy benzaldehydes, respectively. In accordance with above conclusion, we have assigned the theoretically predicted value by the B3LYP/6-311++G(d,p) method at 348 cm^{-1} (mode no: 11) as the C–O–CH_3 angle bending mode, which coincides with the band at 344 cm^{-1} observed in the FT-Raman spectrum. The torsional mode of the O–CH_3 group was observed for anisole at 100 cm^{-1} by some workers.[40–42] Balafour[32] assigned this mode at 82 cm^{-1}, and Lakshmaiah and Rao[34] calculated this mode to be at 58 cm^{-1} for anisole. This mode at 54 cm^{-1} in FT-Raman is assigned to the O–CH_3 torsional mode in our title molecule.

Methyl group vibrations

The title molecule 4M2MBA possesses one CH_3 group in the second position. For the assignments of CH_3 group wavenumbers, one can expect that the nine fundamentals can be associated with each CH_3 group, namely the symmetrical stretching in CH_3 (CH_3 sym. stretching); asymmetrical stretching (i.e. in-plane hydrogen stretching mode); the symmetrical (CH_3 sym. deformation) and asymmetrical (CH_3 asy. deformation) deformation modes; the in-plane rocking (CH_3 ipr), out-of-plane rocking (CH_3 opr) and twisting t(CH_3) bending modes.

The C–H stretching mode in CH_3 occurs at lower wavenumbers than those of the aromatic ring (3000–3100 cm^{-1}). The asymmetric C-H stretching mode of the CH_3 group is expected in the region of 2980 cm^{-1} and the symmetric[43–46] one is expected in the region of 2870 cm^{-1}. For 2-methylpridine, the CH_3 stretching mode is at approximately 3000–2900 cm^{-1}, the in-plane deformations are at 1450–1370 cm^{-1} and the rocking mode is at[1] 1040–900 cm^{-1}. In case of 2-flouro-5-methylbenzonitrile, the CH_3 stretching is at approximately 3000–2890 cm^{-1}, the in-plane deformation is at 1430–1380 cm^{-1} and the rocking mode is at 1020–980 cm^{-1}.[2] In accordance with the above conclusion, the theoretically predicted asymmetric and symmetric stretching vibrations in CH_3 are at 3035, 3011 and 3002 cm^{-1} by the B3LYP/6-311++G(d,p) method (mode nos: 56–54). The FT-IR band at 3006 cm^{-1} represents the asymmetric CH_3 stretching vibration. The counterpart in FT-Raman is at 3007 cm^{-1}. As expected, these three modes are pure stretching modes as is evident from the TED column; they contribute l00%.

For the methylsubstituted benzene derivatives, the asymmetric and symmetric deformation vibrations of the methyl group normally appear in the region of 1465–1440 cm^{-1} and 1390–1370 cm^{-1} respectively.[1–3] The wavenumbers of the modes involving the CH_3 deformation vibrations agree with the commonly accepted region of these vibrations.[46,47] According to the work by Long and Jeorge[48] on 4-methyl pyridine, the wavenumbers at 1041 and 974 cm^{-1} in the FT-Raman spectrum are assigned to the rocking modes of CH_3. The rocking vibrations of the CH_3 group in 4M2MBA appear as independent vibrations. These modes usually appear[31] in the region of 1070–1010 cm^{-1}. The weak band in FT-IR (gas phase) at 931 and a weak band at 926 cm^{-1} in the FT-Raman spectrumare are attributed to the CH_3 rocking mode. The theoretically calculated value by the B3LYP/6-311++G(d,p) method at 948 cm^{-1} shows excellent agreement with the experimental observation. As the CH_3 torsional mode is expected to be below 400 cm^{-1}, the computed bands at 69 and 100 cm^{-1} are assigned to this mode; for the same vibration, the FT-Raman spectral measurements show a very weak band at 54 cm^{-1}.

C–C vibrations

The ring C–C stretching vibrations occur in the region of 1625–1430 cm^{-1}. In general, the bands are of variable intensity and are observed at 1625–1590, 1590–1575, 1540–1470, 1465–1430 and 1380–1280 cm^{-1} from the wavenumber ranges given by Varsanyi[43] for the five bands in this region. In the present work, the wavenumbers observed in the FTIR spectrum at 1610, 1568 and 1507 cm^{-1} have been assigned to C=C stretching vibrations. The C=C corresponding vibrations appear in the FT-Raman spectrum at 1612, 1573 and 1502 cm^{-1}. The same vibrations are observed in the FT-IR gas phase spectrum at 1602 and 1503 cm^{-1}. The theoretically computed values at 1590, 1543 and 1473 cm^{-1} show an excellent agreement with experimental data by the B3LYP/6-311++G(d,p) method (mode nos: 49–47). The TED, corresponding to all C–C vibrations, lies between 30 and 65%, as shown in Table 1, with a combination of C–H in-plane bending in this region. The very strong band at 726 cm^{-1} is observed in the FT-Raman spectrum of 4M2MBA corresponding to the ring-breathing vibration. The theoretically predicted ring-breathing vibration at 720 cm^{-1} by the B3LYP/6-311++G(d,p) method and at 730 cm^{-1} by the HF/6-311++G(d,p) (mode no: 21) coincide with the experimental observation. The TED contribution for this vibration is 43%. The in-plane deformation vibration is at higher wavenumbers than the out-of-plane vibrations. Shimanouchi *et al.*[40] gave the wavenumber data for these vibrations for different benzene derivatives as a result of normal coordinate analysis. The bands observed at 694 and 669 cm^{-1} are assigned to C–C–C deformation vibrations of the phenyl ring. The theoretically computed values at 699, 684, 585, 542 and 442 cm^{-1} by the B3LYP/6-311++G(d,p) (mode nos: 20–18, 15, 13) method are in excellent agreement with the experimental data. The TED contribution for this mode is a mixed mode, as is evident from Table 1.

COOH vibrations

The O–H group in acid gives rise to three vibrations (stretching, in-plane and out-of-plane bending vibrations). The O–H group vibrations are likely to be the most sensitive to the environment, hence they show pronounced shifts in the spectra of the hydrogen-bonded species. The O–H stretching band is characterized by a very broad band appearing approximately at 3400 cm^{-1}. The broad-shoulder band observed at 3354 cm^{-1} in the FTIR solid phase has its origin in the O–H stretching vibration. However, the calculated wavenumber shows a positive deviation of about 284 cm^{-1} by the B3LYP/6-311++G(d,p) method when compared with our experimental data, which may have been due to the presence of strong intermolecular hydrogen bonding. According to TED results, the O–H stretching is a pure mode contributing 100%. The very strong band appearing at 1750 cm^{-1} is assigned as the C=O stretching vibration in the FTIR gas-phase spectrum. The theoretically computed value of 1768 cm^{-1} by the HF/6-311++G(d,p) method shows very good agreement with experimental results. According to TED results, the O–H in-plane and out-of-plane bending vibrations are described as mixed mode vibrations shown in Table 1. The O–H in-plane bending occurs between 1440 and 1395 cm^{-1} and the out-of-plane bending occurs between 960 and 875 cm^{-1}. Strong bands at 1161 cm^{-1} in FT-IR (solid phase), 1178 cm^{-1} in FTIR (gas phase) and 1163 cm^{-1} in FT-Raman are assigned as O–H in-plane bending vibrations and the bands at 576 and 579 cm^{-1} in FTIR (solid phase) and FT-Raman, respectively, are assigned as O–H out-of-plane bending vibrations for the present molecule. The thoretically computed

value of 1170 cm^{-1} (mode no: 34) is in very good agreement for the O-H in-plane bending vibration and this vibration mixes with C–C stretching vibrations. The calculated value of the O–H out-of-plane bending vibration at 575 cm^{-1} (mode no: 17) is also in excellent agreement with experimental one and this vibration also mixes with the C–C–C out-of-plane bending mode. The present assignments agree very well with the values available in the literature.[49–51]

HOMO, LUMO analysis

Many organic molecules that contain conjugated π electrons are characterized as hyperpolarizabilities and were analyzed by means of vibrational spectroscopy.[52,53] In most of the cases, even in the absence of an inversion center, the strongest bands in the Raman spectrum are weak in the IR spectrum and vice versa. The experimental spectroscopic behavior described above is well accounted for by *ab initio* calculations in π-conjugated systems that predict exceptionally large Raman and infrared intensities for the same normal modes.[53] The normal modes of vibrations reveal that the relevant modes can be described as in-plane symmetric stretching vibrations of single C–C bonds, C═O bonds and shrinking of C–C double bonds. These vibrations spread over the whole π-conjugated path with relevant amplitudes from almost all the constituent parts of the molecule, which involves the intramolecular charge transfer from the donor to the acceptor and gives rise to a large variation of the dipole moment, thus gaining a strong infrared activity, on the other hand, in the Raman spectrum. The π-electron cloud movement from donor to acceptor can make the molecule highly polarized through the single–double path when it changes from the ground state to the first excited state. It is also observed in our title molecule that the bands in the FT-IR spectrum when compared with their Raman counterparts show that the relative intensities in IR and Raman spectra result from the electron cloud movement through the π-conjugated framework from the electron donor to the electron-acceptor groups. The analysis of the wave function indicates that the electron absorption corresponds to the transition from the ground to the first excited state and is mainly described by the one-electron excitation from the HOMO to the LUMO. The HOMO, of π nature (i.e. aromatic ring), is delocalized over the whole C–C bond. By contrast, the LUMO is located over the aromatic ring; consequently, the HOMO $\rightarrow$ LUMO transition implies an electron density transfer to methoxy and carboxylic groups from the aromatic ring. Moreover, these orbitals significantly overlap in their position for 4M2MBA. The atomic orbital compositions of the frontier molecular orbital are sketched in Fig. 6.

The HOMO–LUMO energy gap of 4M2MBA was calculated at the B3LYP/6-31(d,p) level and it reveals that the energy gap reflects the chemical activity of the molecule as shown in Table S1 (Supporting Information). LUMO as an electron acceptor represents the ability to obtain an electron, while HOMO represents the ability to donate an electron.

$$\text{HOMO energy} = -0.24845 \text{ a.u.}$$
$$\text{LUMO energy} = -0.04830 \text{ a.u.}$$
$$\text{HOMO–LUMO energy gap} = -0.20015 \text{ a.u.}$$

The calculated self-consistent field (SCF) energy of 4M2MBA is −574.82999 a.u. Moreover, the lowering in the HOMO and LUMO energy gap explains the eventual charge transfer interactions that take place within the molecule.

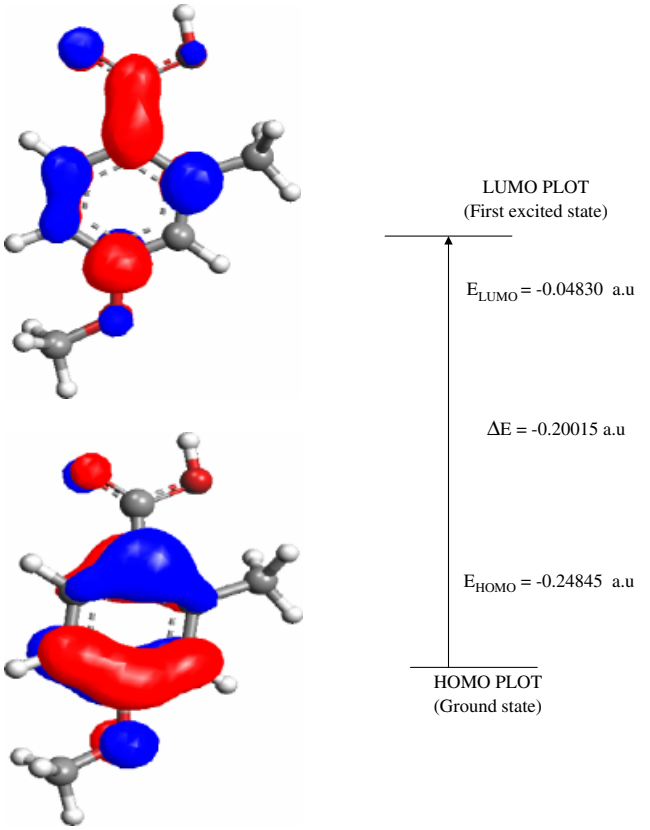

Figure 6. Atomic orbital compositions of the frontier molecular orbital for 4-methoxy-2-methylbenzoic acid.

Conclusions

This paper presents the experimental and theoretical vibrational IR and Raman spectra of the title molecule. The FT-IR (gas and solid phase) and FT-Raman spectra have been recorded in the range of 400–4000 cm^{-1} and 10–3500 cm^{-1}, respectively. Because of the lack of experimental information on the geometric structure available in the literature, theoretical calculations were compared with those of a similar molecule. All observed vibrational bands have been discussed and assigned with the help of TED values on the basis of our calculations. The molecular geometry at all the vibrational wavenumbers of 4M2MBA in the ground state have been calculated by using the HF density functional method at the B3LYP/6-311G(d,p) level. A complete assignment of the fundamentals was proposed on the basis of the TED calculations. Furthermore, the thermodynamic, non-linear optical, first-order hyperpolarizabilities and total dipole moment properties of the compound have been calculated in order to get an insight into the compound. We hope that the results are of assistance in the quest for experimental and theoretical evidence for the title molecule is reaction intermediates and for non-linear optical and photo-elastic materials.

Acknowledgements

The visit of Dr N. Sundaraganesan to Ahi Evran University was facilitated by the Scientific and Technical Research council of Turkey (TUBITAK) BIDEB-2221.

Dr C. Meganathan was supported by a fellowship from the BK21 program, Ministry of Education and Human Resources

Development, Korea and this work was supported by grants from the MOST/KOSEF for the EB-NCRC (grant # R15-2003-012-02001-0).

Supporting information

Supporting information may be found in the online version of this article.

References

[1] N. Sundaraganesan, S. Illakiamani, B. Dominic Joshua, *Spectochim. Acta* **2007**, *67A*, 287.
[2] M. A. Palafox, M. Gil, J. L. Nunez, *Vib. Spectrosc.* **1993**, *6*, 95.
[3] R. Swinslocka, M. Samsonowicz, E. Regulaska, W. Lewandowski, *J. Mol. Struct.* **2006**, *792*, 227.
[4] N. Sundaraganesan, B. Anand, C. Meganathan, B. Dominic Joshua, *Spectrochim. Acta* **2008**, *69A*, 871.
[5] C. K. Lyndon, R. A. Klein, J. P. Coleman, *(Dept of Microbiology and immunology, East Carolina University Green ville, vc 27858 USA), Liquids* **1995**, *39*(9), 863.
[6] P. Mani, PhD Thesis, Pondicherry University, **2004**, 107.
[7] M. Samsonowics, T. Hrynaszkiewicz, R. S. Wislocka, E. Regulska, W. Lewandowski, *J. Mol. Struct.* **2005**, *345*, 744.
[8] C. Shou-Yihwanf, Y. Chou, N. T. Liang, *J. Raman Spectrosc.* **1988**, *19*, 365.
[9] K. Furic, J. R. Durig, *Chem. Phys. Lett.* **1986**, *126*, 92.
[10] P. K. Verma, A. Rashid, S. Tariq, *Indian J. Pure Appl. Phys.* **1987**, *25*, 203.
[11] M. Chapman, P. K. Verma, *Indian J. Phys.* **2003**, *77B*, 315.
[12] V. K. Rastogi, M. P. Rajpoot, S. N. Sharma, *Indian J. Phys.* **1984**, *58B*, 311.
[13] S. Ahamed, S. Mathew, P. K. Verma, *Indian J. Pure Appl. Phys.* **1992**, *30*, 764.
[14] N. Sundaraganesan, B. Dominic Joshua, T. Radjakoumar, *Indian J. Pure Appl. Phys.* **2009**, *47*, 248.
[15] M. J. Frisch, W. Trucks, H. B. Schlegel, G. E. Scuseria, M. A. Robb, J. R. Cheeseman, J. A. Montgomery, Jr., T. Vreven, K. N. Kudin, J. C. Burant, J. M. Millam, S. S. Iyengar, J. Tomasi, V. Barone, B. Mennucci, M. Cossi, G. Scalmani, N. Rega, G. A. Petersson, H. Nakatsuji, M. Hada, M. Ehara, K. Toyota, R. Fukuda, J. Hasegawa, M. Ishida, T. Nakajima, Y. Honda, O. Kitao, H. Nakai, M. Klene, X. Li, J. E. Knox, H. P. Hratchian, J. B. Cross, C. Adamo, J. Jaramillo, R. Gomperts, R. E. Stratmann, O. Yazyev, A. J. Austin, R. Cammi, C. Pomelli, J. W. Ochterski, P. Y. Ayala, K. Morokuma, G. A. Voth, P. Salvador, J. J. Dannenberg, V. G. Zakrzewski, S. Dapprich, D. Daniels, M. C. Strain, O. Farkas, D. K. Malick, A. D. Rabuck, K. Raghavachari, J. B. Foresman, J. V. Ortiz, Q. Cui, A. G. Baboul, S. Clifford, J. Cioslowski, B. B. Stefanov, G. Liu, A. Liashenko, P. Piskorz, I. Komaromi, R. L. Martin, D. J. Fox, T. Keith, M. A. Al-Laham, C. Y. Peng, A. Nanayakkara, M. Challacombe, P. M. W. Gill, B. Johnson, W. Chen, M. W. Wong, C. Gonzalez, J. A. Pople, *Gaussian 03 Program*, Gaussian Inc.: Wallingford, CT, **2004**.
[16] H. B. Schlegel, *J. Comput. Chem.* **1982**, *3*, 214.
[17] J. Baker, A. A. Jarzccki, P. Pulay, *J. Phys. Chem.* **1998**, *102A*, 1412.
[18] P. Pulay, J. Baker, K. Wolinski, Green Arc Road, Suite A, Fayettevile, AR72703, USA, **2013**.
[19] G. Keresztury, S. Holly, J. Varga, G. Besenyei, A. Y. Wang, J. R. Durig, *Spectrochim. Acta* **1993**, *49A*, 2007.
[20] G. Keresztury, J. M. Chalmers, P. R. Griffith (Eds), *Raman Spectroscopy: Theory, in Hand book of Vibrational Spectroscopy*, vol. 1, John Wiley &Sons Ltd.: New York, **2002**.
[21] D. A. Kleinman, *Phys. Rev.* **1962**, *126*, 1977.
[22] R. F. Bryan, D. H. White, *Acta Crystallogr.* **1982**, *38B*, 1014.
[23] M. Kurt, M. Yurdakul, S. Yurdakul, *J. Mol. Struct. (Theochem)* **2004**, *71*, 25.
[24] A. C. Dros, R. W. J. Zijlstra, P. T. Van Duijnen, A. L. Spek, H. Kooijman, R. M. Kellogg, *Tetrahedron* **1998**, *54*, 7787.
[25] F. Takusagawa, A. Shimada, *Acta Crystallogr.* **1976**, *32B*, 1925.
[26] A. Kutoglu, C. Scheringer, *Acta Crystallogr., Sect. C (Cr. Str. Comm.)* **1983**, *39*, 232.
[27] G. A. Jaffrey, *An Introduction to Hydrogen Bonding*, Oxford University Press: USA, **1997**, p 32.
[28] P. Pulay, G. Fogarasi, G. Pongor, J. E. Boggs, A. Vargha, *J. Am. Chem. Soc.* **1983**, *105*, 7037.
[29] A. P. Scott, L. Radom, *J. Phys. Chem.* **1996**, *100*, 16502.
[30] V. K. Rastogi, M. A. Palafox, R. P. Tanwar, L. Mittal, *Spectrochim. Acta* **2002**, *A58*, 1989.
[31] M. Silverstein, G. Clayton Basseler, C. Morill, *Spectrometic Identification of Organic Compounds*, Wiley: New York, **1981**.
[32] J. W. Balfour, *Spectrochim. Acta.* **1983**, *39A*, 795.
[33] B. Lakshmaiah, G. Ramana Rao, *J. Raman Spectrosc.* **1989**, *20*, 439.
[34] B. Lakshmaiah, G. Ramana Rao, *Indian J. Pure Appl. Phys.* **1991**, *29*, 370.
[35] B. Venkataram Reddy, G. Ramana Rao, *Vib. Spectrosc.* **1994**, *6*, 231.
[36] V. Ashok Babu, B. Lakshmaiah, K. Sree Ramulu, G. Ramana Rao, *Indian J. Pure Appl. Phys.* **1987**, *25*, 58.
[37] N. L. Owen, R. E. Hester, *Spectrochim. Acta* **1969**, *25A*, 343.
[38] G. E. Campagnaro, J. L. Wood, *J. Mol. Struct.* **1970**, *6*, 117.
[39] D. N. Sing, R. A. Yadav, *Assian Chem. Lett.* **1998**, *2*, 65.
[40] T. Shimanouchi, Y. Kakiuti, I. Gamo, *J. Chem. Phys.* **1956**, *25*, 1245.
[41] L. D. Pietila, B. Mannfors, K. Palmo, *Spectrochim. Acta* **1988**, *44A*, 141.
[42] V. Krishnakumar, R. John Xavier, *Spectrochim. Acta* **2005**, *61A*, 253.
[43] G. Varsanyi, *Vibrational Spectra of Benzene Derivatives*, Academic Press: New York, **1969**.
[44] D. A. Kleinman, *Phy. Rev.* **1962**, *126*, 1977.
[45] B. Smith, *Infrared Spectral Interpretation, A Systematic approach*, CRC Press: Washington, DC, **1999**.
[46] N. B. Colthup, L. H. Daly, S. E. Wiberly, *Introduction to Infrared and Raman spectroscopy*, Academic Press: New York, **1990**.
[47] J. F. Areanas, I. Lopez Tocn, J. C. Otero, J. I. Marcos, *J. Mol. Struct.* **1997**, *410*, 433.
[48] D. A. Long, W. O. Jeorge, *Spectrochim. Acta* **1963**, *19*, 1777.
[49] J. Marshal, *Indian J. Phys.* **1998**, *72B*, 661.
[50] S. Thakur, V. P. Gupta, *Indian J. Pure Appl. Phys.* **1998**, *36*, 567.
[51] T. Syed, P. K. Verma, *Indian J. Phys.* **1983**, *57B*, 413.
[52] Y. Atalay, D. Avci, A. Başoğlu, *Struct. Chem.* **2008**, *19*, 239.
[53] T. Vijayakumar, I. Hubert Joe, C. P. R. Nair, V. S. Jayakumar, *Chem. Phys.* **2008**, *343*, 83.